Research Article

Muhammad Razlan Zakaria, Hazizan Md Akil*, Mohd Firdaus Omar, Mohd Mustafa Al Bakri Abdullah, Aslina Anjang Ab Rahman, and Muhammad Bisyrul Hafi Othman

Improving flexural and dielectric properties of carbon fiber epoxy composite laminates reinforced with carbon nanotubes interlayer using electrospray deposition

https://doi.org/10.1515/ntrev-2020-0090
received September 25, 2020; accepted October 4, 2020

Abstract: The electrospray deposition method was used to deposit carbon nanotubes (CNT) onto the surfaces of woven carbon fiber (CF) to produce woven hybrid carbon fiber–carbon nanotubes (CF–CNT). Extreme high-resolution field emission scanning electron microscopy (XHR-FESEM), X-ray diffraction (XRD), Raman spectroscopy and Fourier transform infrared spectroscopy (FT-IR) were used to analyze the woven hybrid CF–CNT. The results demonstrated that CNT was successfully and homogenously distributed on the woven CF surface. Woven hybrid CF–CNT epoxy composite laminates were then prepared and compared with woven CF epoxy composite laminates in terms of their flexural and dielectric properties. The results indicated that the flexural strength, flexural modulus and dielectric constant of the woven hybrid CF–CNT epoxy composite laminates were improved up to 19, 27 and 25%, respectively, compared with the woven CF epoxy composite laminates.

Keywords: carbon fiber, carbon nanotube, hybrid material, epoxy composite laminates

1 Introduction

Carbon fiber (CF) epoxy composite laminates exhibit high strength and modulus to weight ratio and are broadly used in the aerospace, automobile industries, military, electronic and sporting goods [1]. The CF epoxy composite laminates have also gone through a level of maturity beyond the laboratory stage [2]. Even though the CF epoxy composite laminates have been widely used in many applications, their potential is still governed by few factors. As is well known, the CF epoxy composite laminates in the form of laminates have poor performance in the direction of through thickness [3]. This is due to the inert and non-polar structure of the CF, and their low wettability, which result in poor interfacial adhesion between the fiber and the matrix [4]. To offer better designs of CF epoxy composite laminates for advanced components, significant enhancements are necessary with regard to the aforementioned properties. The incorporation of nanofiller, such as carbon nanotubes (CNT), into the CF epoxy composite laminates has been developed as an efficient method for improving the fiber/matrix interfacial adhesion, including mechanical interlocks, chemical bonding and enhancing the performance especially in the direction of through thickness [5]. In addition, the extraordinary mechanical and physical properties of CNT have inspired their utilization as additives to enhance the inadequate properties of CF epoxy composite laminates [6]. CNT is one-dimensional with a cylindrical nanostructure of sp^2 hybridized carbon atoms that are densely packed in a honeycomb crystal lattice [7]. CNT has been reported to possess superior mechanical properties, with Young's modulus of 0.27–0.95 TPa and tensile strengths of 11–63 GPa [8]. CNT is also expected to offer remarkable performances in areas such

* **Corresponding author: Hazizan Md Akil,** School of Materials and Mineral Resources Engineering, Engineering Campus, Universiti Sains Malaysia, 14300 Nibong Tebal, Pulau Pinang, Malaysia, e-mail: hazizan@usm.my
Muhammad Razlan Zakaria, Mohd Firdaus Omar, Mohd Mustafa Al Bakri Abdullah: Faculty of Chemical Engineering Technology, Universiti Malaysia Perlis (UniMAP), Perlis, Malaysia; Geopolymer & Green Technology, Centre of Excellent (CEGeoGTech), Universiti Malaysia Perlis (UniMAP), Perlis, Malaysia
Aslina Anjang Ab Rahman: School of Aerospace Engineering, Engineering Campus, Universiti Sains Malaysia, 14300 Nibong Tebal, Pulau Pinang, Malaysia
Muhammad Bisyrul Hafi Othman: School of Chemical Sciences, Universiti Sains Malaysia, 11800 Minden, Penang, Malaysia

as thermal and electrical properties [9]. Thermal and electrical conductivity of CNT is up to 3,000 W/mK and 1,800 S/cm, respectively [10].

There are two common ways for incorporating CNT into the CF epoxy composite laminates. First, CNT is used as reinforcing fillers in the epoxy matrix of the CF epoxy composite laminates to improve their performance [11]. The challenge of this approach is that the uniform dispersion of CNT in the epoxy matrix is difficult to achieve, especially at high concentrations, due to the dramatically increased viscosity of the resin [12]. Highly viscous resin with agglomerated CNT is very difficult to process and always leads to poor performance of CF epoxy composite laminates. In addition, the direct incorporation of the CNT into the epoxy matrix is less effective in improving the interfacial bonding between the CF and epoxy matrix [13].

Another way is to grow or deposit CNT directly onto CF surface to form a hierarchical reinforcement. In the past, several methods were successfully developed to produce hybrid carbon fiber–carbon nanotube (CF–CNT) such as chemical vapour deposition (CVD) [14], electrophoretic deposition (EPD) [15] and chemical functionalization [16]. Although all these methods are widely reported to have successfully hybridized CF with CNT, each method has some drawbacks. In the case of the CVD method, the high processing temperature leads to the degradation of the properties of the CF in the longitudinal direction [17]. Furthermore, the metal catalysts used for growing the CNT can also cause contamination, and it is difficult to use the CVD method for large-scale production [18]. In the case of EPD and chemical functionalization, although both methods are carried out at room temperature, these methods expose the CF and CNT to oxidation [19], which can damage the structure of the CF and CNT and lead to the degradation of the mechanical properties of the CF epoxy composite laminates [20].

The electrospray deposition (ESD) method is another promising method for the hybridization of CF and CNT [21]. This method is carried out at room temperature and no oxidation treatment is performed on the CF and CNT [22]. In addition, epoxy resin is used as a binder to strengthen the adhesion between the CF and CNT. Furthermore, this method is used in high-electric fields to convert suspension or liquid into non-agglomerating nano or microdroplets of uniform sizes and suitable to produce micrometer-thin or thinner layers of spray with uniform coating. Besides, there are also a few other advantages to this method such as cost-effectiveness, simplicity and its suitability for large-scale production [23].

In addition, epoxy composites are also of great interest to be used in advanced electrical materials, as they have good physical and mechanical properties [24]. However, the dielectric constant of epoxy resin is relatively low. Therefore, by using conductive filler such as hybrid CF–CNT can dramatically improve the dielectric properties of epoxy composites. Yao et al. have studied the dielectric properties of hybrid CF–CNT reinforced epoxy composites and reported an improvement in dielectric properties due to the impressive hierarchical structure of the hybrid CF–CNT [25]. Similar increasing trends in dielectric properties have also been reported by Wang et al., which obtained hybrid CF–CNT by in situ growth of CNT on CF by CVD [18].

Therefore, this paper studied the use of ESD in the production of woven hybrid CF–CNT. The woven hybrid CF–CNT that was produced using this method was characterized by extreme high-resolution field emission scanning electron microscopy (XHR-FESEM), high resolution transmission electron microscopy (HRTEM), X-ray diffraction (XRD), Raman spectroscopy and Fourier transform infrared spectroscopy (FT-IR). Then, woven hybrid CF–CNT epoxy composite laminates were fabricated using vacuum-assisted resin transfer moulding to produce samples with a good finish to ensure the reliability of the test. Finally, the flexural and dielectric properties of the woven hybrid CF–CNT epoxy composite laminates were studied.

2 Experimental

2.1 Materials

Multiwalled CNT (with a length of 10–30 μm, inner diameter of 5–10 nm, and outer diameter of 20–30 nm) and woven CF (thickness of 0.3 mm) were purchased from Sky Spring Nanomaterials Inc., Houston, TX, USA and Toray Industries Inc., Chuo-Ku, Tokyo, respectively. An epoxy adhesive (UV 367) was purchased from Penchem Technologies Sdn. Bhd., Penang, Malaysia. EpoxAmite 100 resin and EpoxAmite 103 slow hardener for epoxy composite laminates were purchased from Smooth-On, Inc., Macungie, PA, USA. *N*-Methyl-2-pyrrolidone (NMP) solvent was purchased from Sigma-Aldrich, St. Louis, MO, USA.

2.2 Preparation of woven hybrid CF–CNT

Woven hybrid CF–CNT was prepared using the ESD method. A sonicator (Q700, Qsonica, Melville, CT, USA)

was used to disperse 0.1 g of CNT in 50 mL of NMP at a frequency of 50 kHz for 5 h to prepare a CNT dispersion that was appropriate for the ESD. The sonicator was used to break down the CNT agglomeration and produce a better CNT distribution. Then , 1 mL of UV 367 was added to the CNT dispersion as a binder to increase the binding strength between the CNT and woven CF.

Then, the woven CF was mounted onto a steel roller, which was connected to the ground electrode, in preparation for the ESD. The speed of the steel roller was fixed at 120 rpm. A 20 mL syringe was then filled with the CNT dispersion and was placed tightly on a precision syringe pump (Model NE-1600, New Era Pump Systems Inc., Farmingdale, NY, USA). The precision syringe pump was positioned on the adjustable plate, which moved to the right and left at a speed of 0.5 rpm to ensure that the CNT spray reached all parts of the woven CF. The syringe was then fitted with a flat-end stainless steel nozzle (internal diameter 0.26 mm, length 38 mm) and wired to a high-voltage power supply (Model ES20P-20W, Gamma High Voltage Research Inc., Ormond Beach, FL, USA). Finally, a UV lamp, as the source of UV light, was set up above the steel roller to ensure that the UV367 was cured after the spray process. Figure 1 shows a general view of the ESD setup.

The CNT dispersion with a flow rate of 0.02 mL/min was applied throughout the process with an applied voltage of 15 kV and spray duration of 15 min. On completion of the spray process, the woven CF was left to dry for 24 h, and the spray process was repeated on the opposite side.

2.3 Characterization of woven hybrid CF–CNT

An extreme high-resolution field emission scanning electron microscope (XHR-FESEM) (Model: FEI Verios 460 L) was used to analyze the morphology of the woven hybrid CF–CNT. X-ray diffraction (XRD) was performed using a D8 Diffractometer (Bruker-AXS) to investigate the crystallographic structures of the CNT, woven CF and woven hybrid CF–CNT in the 2θ range of 10°–80°. Raman spectroscopy (Renishaw inVia Raman spectrometer) was used to investigate the structural characteristics of the CNT, woven CF and woven hybrid CF–CNT. Fourier transform infrared spectroscopy (FT-IR) (Spectrum One, PerkinElmer) was performed to investigate the presence of functional groups in the CNT, woven CF and woven hybrid CF–CNT.

2.4 Preparation of woven hybrid CF–CNT epoxy composite laminates via vacuum-assisted resin transfer moulding (VARTM)

VARTM was used to prepare the woven hybrid CF–CNT epoxy composite laminates. The two-part flat rectangular mould, with dimensions of 300 mm × 210 mm × 2.5 mm, was made of glass fiber epoxy composites. The mould was coated with a thin layer of silica to ensure the high

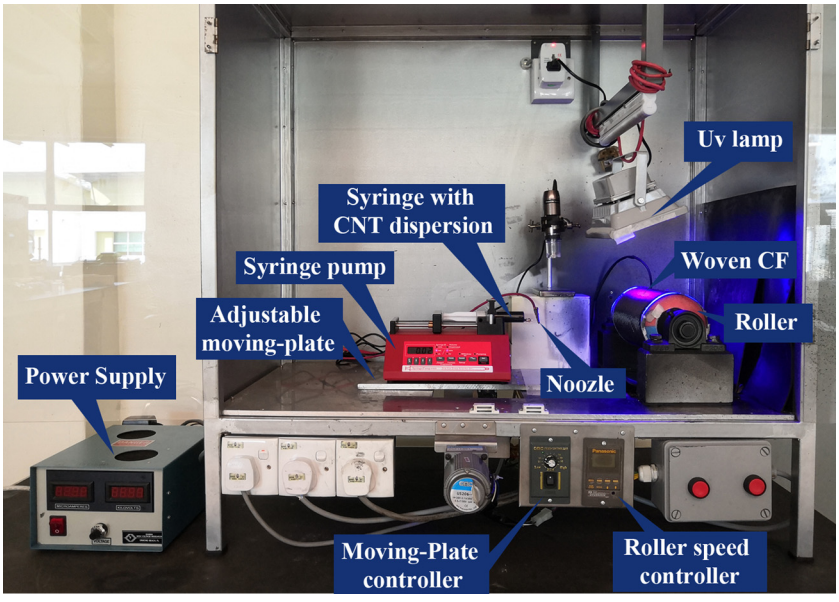

Figure 1: General view of the electrospray deposition process.

surface quality of the manufactured woven hybrid CF–CNT epoxy composite laminates. In order to provide a proper seal to the mould, a rubber gasket was placed around the perimeter of the mould halves. Eight layers of woven hybrid CF–CNT were then stacked together inside the mould cavity to form a 2.5 mm thick plate. The EpoxAmite 100 resin and EpoxAmite 103 slow hardener were prepared by mixing them at a mass ratio of 100:28.4. A vacuum was applied to the mould to provide the required pressure to force the epoxy suspension into the preform. No gaps were present between the edges of the mould and the woven hybrid CF–CNT preform to prevent the epoxy suspension from flowing outside the preform to the vacuum port. To start the VARTM process, the inlet line was opened and the epoxy resin was free to infiltrate into the preform. The infiltration of the epoxy suspension was aided by the atmospheric pressure, which pushed the epoxy suspension through the preform into the space evacuated by the vacuum pump. The epoxy suspension was allowed to flow across the fiber layers in the direction of the thickness. Any excess epoxy suspension that flowed through the outlet line was captured in a resin trap. The vacuum pump was left running during the process, which lasted for about 20 min, to facilitate the infiltration of the epoxy suspension. After the mould had been fully infiltrated with the epoxy suspension, both the inlet and outlet were closed and maintained under a constant vacuum of 75 cmHg. The vacuum was discontinued after the epoxy suspension had been cured and the woven hybrid CF–CNT epoxy composite laminate part had been de-moulded. The same process was used to prepare woven CF epoxy composite laminates. The description of the samples is given in Table 1.

2.5 Characterization of woven hybrid CF–CNT epoxy composite laminates

The flexural properties of the CF/epoxy and CF–CNT/epoxy were investigated using a universal testing machine (Model: 5982, Instron, USA) according to ASTM D 790. The test was performed with the span length maintained at 40 mm and at a crosshead speed of 2 mm/min. At least three specimens were tested for each case to ensure the reliability of the test results. The fractured surfaces of the CF/epoxy and CF–CNT/epoxy specimens were characterized using XHR-FESEM (Model: FEI Verios 460 L). The fractured surfaces of the CF/epoxy and CF–CNT/epoxy were coated with a thin layer of gold to improve their conductance for observations using FESEM. Dielectric properties of the CF/epoxy and CF–CNT/epoxy were measured using Agilent 4284A LCR meter at room temperature over a frequency range from 1 kHz to 1 MHz. The dielectric test samples were cut from the CF/epoxy and CF–CNT/e/epoxy panel with dimension of 30 mm (length), 30 mm (width) and 2.5 mm (thickness).

Table 1: Description of the samples

Sample	Description
CF/epoxy	Epoxy reinforced with 8 layers of woven CF
CF–CNT/epoxy	Epoxy reinforced with 8 layers of woven hybrid CF–CNT

3 Results and discussion

The surface morphologies of the CF, CNT and hybrid CF–CNT were characterized by using FESEM. Figure 2a displays the morphological structure of the CF with diameter about 6–8 μm. In addition, The smooth surface of CF with grooves running along the longitudinal direction can also be clearly seen. Figure 2b shows the morphological structure of the CNT in the form of tubular with diameter about 10–20 nm.

Figure 3 shows the FESEM images of the hybrid CF–CNT. It was observed that the CNT was homogeneously distributed and covered the entire surface of the CF. In addition, the ESD method also deposits the CNT without forming any agglomeration on the CF surface.

A diffraction pattern is generated when X-rays interact with a crystalline substance. The XRD pattern of a pure substance can be used to identify the substance because the same substance always gives the same pattern [26]. Thus, the crystalline form of the hybrid CF–CNT was investigated using XRD to examine the effect of the CNT deposition on the CF surface. As is well known, the main features of the XRD patterns of CNT and CF are close to those of graphite due to their intrinsic nature. Figure 4 shows the XRD patterns of CNT, CF and the hybrid CF–CNT. As can be seen from the figure, all the samples displayed the existence of carbon. This was due to the presence of the (002) peak of graphite at 25.84°. The intensity and broadness of the (002) peak were influenced by the ordered graphitic structure of the CNT and CF. Based on the result, the CNT showed a narrow and higher (002) peak compared to the CF. This indicated that the CNT had a highly ordered and well-oriented graphitic

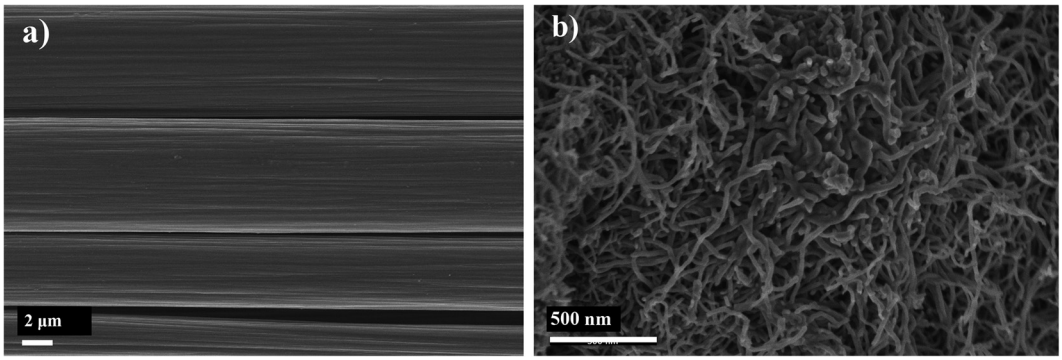

Figure 2: SEM images of (a) CF and (b) CNT.

structure. In addition, the XRD pattern of the CNT showed the presence of a second peak corresponding to the (100) peak at 42.85°, which was also indexed to the hexagonal graphitic structure of CNT [27]. For the hybrid CF–CNT, the deposition of CNT on the CF caused the intensity of the (002) peak to be between the intensity of the CNT and CF. Meanwhile, the presence of the (100) peak in the XRD pattern of the CNT could not be significantly observed in the XRD pattern of the hybrid CF–CNT. This may have been due to the small amount of CNT deposited on the surface of the large CF structure.

The Raman spectroscopy of the CNT, CF and hybrid CF–CNT was undertaken at room temperature with a wavelength of 633 nm. The Raman spectroscopy is frequently employed to study the different structural characteristics of carbon structures such as CNT and CF. It is a useful tool for examining nanocrystalline, crystalline and amorphous graphitic base materials [28]. Hence, it can provide a much better understanding of the effect of the deposition of CNT on the CF surface. Figure 5 displays the representative Raman spectra of the CNT, CF and hybrid CF–CNT. The most intense features in the Raman spectra were the D-band (at 1,350 cm^{-1}), G-band (at 1,500–1,600 cm^{-1}) and G*-band (at ~2,600 cm^{-1}) [29]. The D-band represented the defects in the graphitic structure and disordered carbon, the G-band represented the

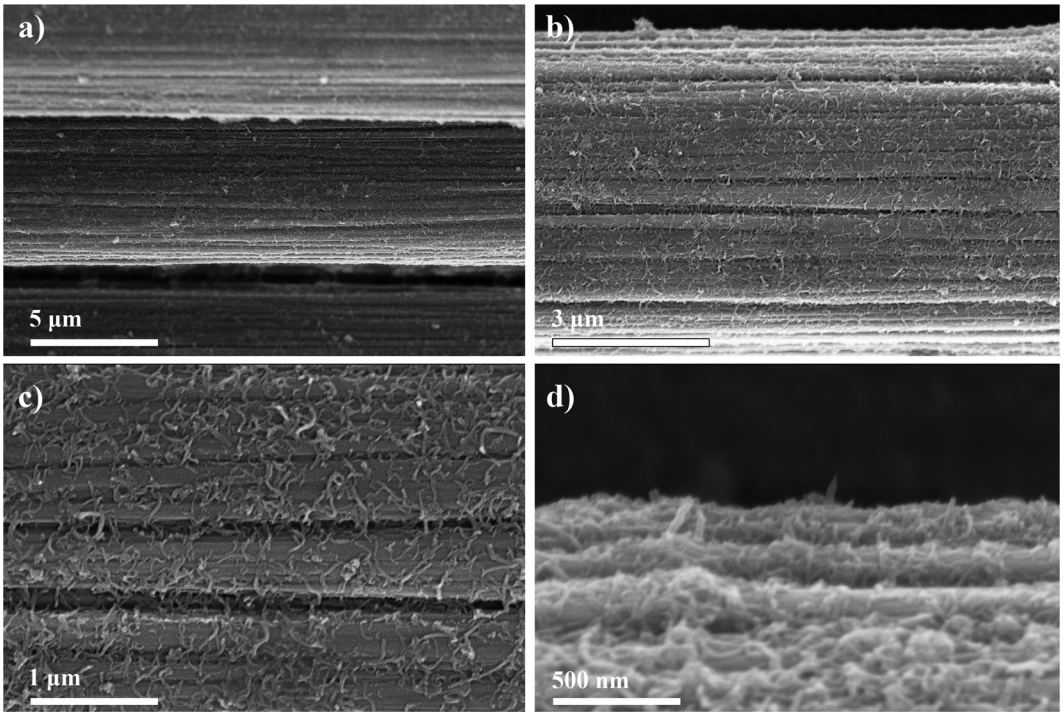

Figure 3: SEM images of hybrid CF–CNT with magnifications of (a) 20,000×, (b) 40,000×, (c) 1,00,000×, and (d) 2,00,000×.

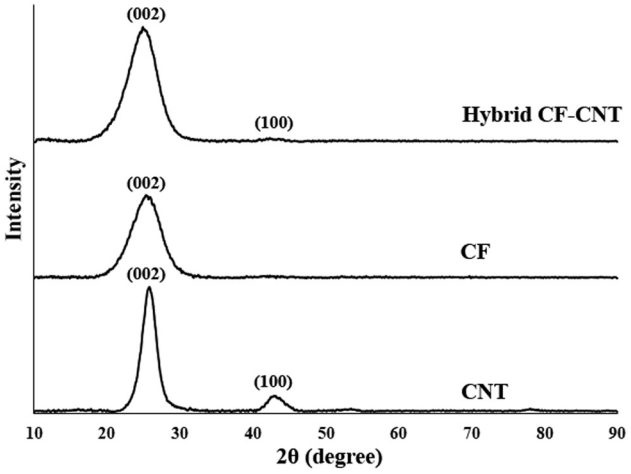

Figure 4: XRD patterns of CNT, CF and hybrid CF–CNT.

crystalline graphitic structure, and the tangent vibrations of sp^2 carbon, and the G*-band represented the stacking order of the graphene layers [30]. There are several factors that contribute to disorders and defects in a graphitic structure such as vacancies, heteroatoms, heptagon–pentagon pairs and kinks [31]. A common method for measuring the quality of samples is to analyze the ratio of the intensity of the D-band to the G-band (I_D/I_G). Usually, materials with a low I_D/I_G ratio are sp^2 bonded carbon atoms with a few defects or high purity [32]. Large quantities of impurities or defects in a sample are indicated by a high I_D/I_G ratio. Based on Table 2, the I_D/I_G ratios of the CNT, CF and hybrid CF–CNT were calculated as 1.69, 0.75 and 1.30, respectively. From the results, the CNT showed a higher I_D/I_G ratio compared to the CF. This

Table 2: Raman intensities of CNT, CF and hybrid CF–CNT

Intensity	I_D	I_G	I_{G*}	I_D/I_G	I_{G*}/I_G
CNT	3967.65	2343.75	1428.44	1.69	0.61
CF	486.60	650.10	—	0.75	—
Hybrid CF–CNT	1497.57	1149.66	881.66	1.30	0.77

may have been due to some kinks or twists in the CNT structure, which gave rise to the high intensity of the D-band [33]. Although the CNT showed a higher I_D/I_G ratio compared to the CF, it showed a significantly higher G-band peak compared to the CF. This indicated that the CNT had a more graphitic structure than the CF. The effect of the deposition of CNT on the CF surface could be observed in the Raman spectrum for the hybrid CF–CNT.

The presence of a G*-band in a Raman spectrum indicates the presence of a graphene layer [34]. From the results, the Raman spectrum for the CNT indicated the presence of a G*-band, while the Raman spectrum for the CF showed the absence of a G*-band. This was because the CNT was actually the graphene sheet that had been rolled into a cylindrical shape. Thus, the presence of a G*-band in the hybrid CF–CNT indicated that the CNT had been successfully deposited on the CF surface. In addition, the G*-band was also used to investigate the number of CNT layers. In principle, the ratio of the intensity of the G*-band to the intensity of the G-band (I_{G*}/I_G) can be calculated to determine the number of CNT layers. A higher number of CNT layers will result in a lower I_{G*}/I_G ratio. The CNT is multi-layered or multi-walled if the I_{G*}/I_G is lower than 1 [35]. Based on the

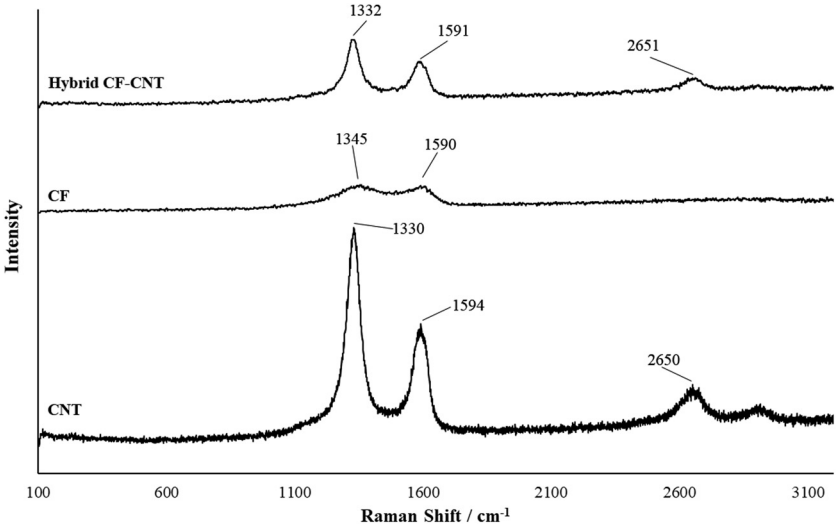

Figure 5: Raman spectra of CNT, CF and hybrid CF–CNT.

result, the I_{G*}/I_G intensity ratios of CNT and the hybrid CF–CNT were 0.61 and 0.77, respectively. The result showed that there was no significant difference between the I_{G*}/I_G of CNT and the hybrid CF–CNT, thereby indicating that the CNT in both samples was multiwalled CNT.

The Fourier transform infrared spectroscopy (FT-IR) is a structural spectroscopic technique that is used to characterize and identify the bonding structure of atoms based on the IR radiation interaction with matter. It measures the radiation frequencies at which a substance absorbs, and it results in the production of vibrations in the molecules [36]. Figure 6 shows the FT-IR spectra of CNT, CF and hybrid CF–CNT. All the samples produced almost a similar spectrum due to the graphitic carbon base structure of CNT and CF. The CNT and CF consisted of hexagonal aromatic rings of hybridized sp^2 carbon atoms. The difference between the FT-IR spectrums of each sample was only in their characteristics such as the broadness and sharpness of the peaks, which indicated the concentration or number of functional groups in the samples. Based on the result, the FT-IR spectrum of CNT showed the presence of peaks at 1,625 cm^{-1} (C=C stretching), 2,920 cm^{-1} (C–H stretching) and 3,430 cm^{-1} (O–H stretching). Meanwhile, the FT-IR spectra of CF and the hybrid CF–CNT showed the presence of peaks at 1,420 cm^{-1} (C–O stretching), 1,625 cm^{-1} (C=C stretching), 2,920 cm^{-1} (C–H stretching) and 3,430 cm^{-1} (O–H stretching). The C=C stretching was due to the sp^2 hybridized carbon atoms from the CNT and CF [37]. The CNT showed a high intensity at the 1,625 cm^{-1} peak, which indicated the presence of more C=C bonds compared to the CF. This means the CNT had more hexagonal aromatic rings in its graphitic structure than CF. This statement was also supported by previous Raman spectra that demonstrated that CNT had a higher G-band intensity compared to CF. The peak at 2,920 cm^{-1} was assigned to the symmetric and asymmetric stretching vibrations of the C–H bonds from the aliphatic chain [36]. The presence of these peaks in the FT-IR spectrum represented the amorphous structure and impurities in the CNT and CF [38]. From the FT-IR spectrum, all three samples showed a low intensity at the peak at 2,920 cm^{-1}, which indicated an amorphous structure and a small amount of impurities in the CNT, CF and hybrid CF–CNT. The peak at 1,042 cm^{-1} (C–O stretching) was only found on the FT-IR spectra of the CF and hybrid CF–CNT. This C–O bond may be associated with polymer sizing from the CF since the CF was used as received. The polymer sizing used for this type of CF is based on epoxy. Thus, the presence of the C–O bond on the FT-IR spectrum of CF and the hybrid CF–CNT may originate from the C–O of the epoxy structure. The hydroxyl (O–H) groups were determined at the stretching mode in the range of 3,000–4,000 cm^{-1}. The presence of a peak centred at 3,430 cm^{-1} was due to the hydroxyl group from the intermolecular hydrogen-bonded OH–OH or the possibility of adsorbed water. From the FT-IR spectrum of the hybrid CF–CNT, the effect of the CNT deposition on the CF surface could be observed, where the intensity of the CF peaks at 1,625 and at 3,430 cm^{-1} had increased.

In addition, this FT-IR spectrum analysis also demonstrated the absence of the C=O stretching vibration mode at the peaks in the range of 1,650–1,800 cm^{-1} for all the samples. Generally, the C=O stretching represents the carboxyl groups as a result of the oxidation of carbon due to the oxidative process such as strong acid treatment (nitric and sulphuric acid) or thermal oxidation at a high temperature. Since no peak was found in the range of 1,700–1,800 cm^{-1} for the hybrid CF–CNT FT-IR spectrum,

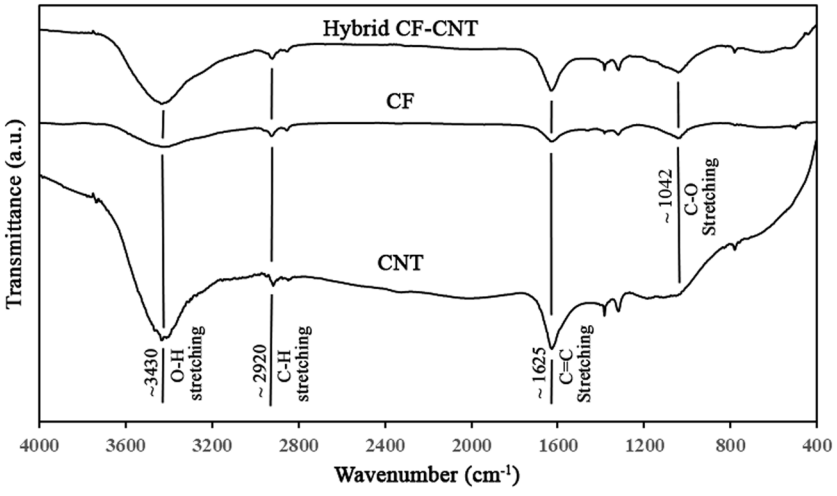

Figure 6: FT-IR spectra of CNT, CF and hybrid CF–CNT.

it indicated that the ESD method did not cause any oxidation at the surface of the CNT and CF compared to other hybridization methods such as CVD, EPD and chemical functionalization, as mentioned in the literature review [21].

Flexural properties can also be considered as important for the assessment of mechanical properties under bending conditions. Figure 7 presents the flexural stress–strain curves of the CF/epoxy and CF–CNT/epoxy. As shown in the figure, the flexural stress linearly increased with flexural strain up to the maximum level of flexural stress. The maximum stress in the respective stress–strain curves was described as the ultimate flexural strength in each case. The comparison of the ultimate flexural strength between the CF/epoxy and CF–CNT/epoxy is shown in Figure 8a. Based on the result, it can be seen that the CF–CNT/epoxy showed a higher ultimate flexural strength compared to the CF/epoxy. The CF–CNT/epoxy demonstrated an ultimate flexural strength of 674 MPa, showing an increase of 19% compared to that of CF/epoxy. This increasing trend was also in accordance with the findings of other researchers such as Yao et al. [39] and Zhao et al. [40], who reported an improvement of about 20 and 18%, respectively, in the ultimate flexural strength. The improvement of the ultimate flexural strength of the CF–CNT/epoxy could have been related to the significant presence of the CNT on the CF surface, which also shared the stress transfer along with the CF [41]. This situation demonstrated that in the case of the CF–CNT/epoxy, the deposition of CNT on the CF surface introduced a strong 3D network that efficiently improved the stress transfer between the CF and the epoxy matrix [42].

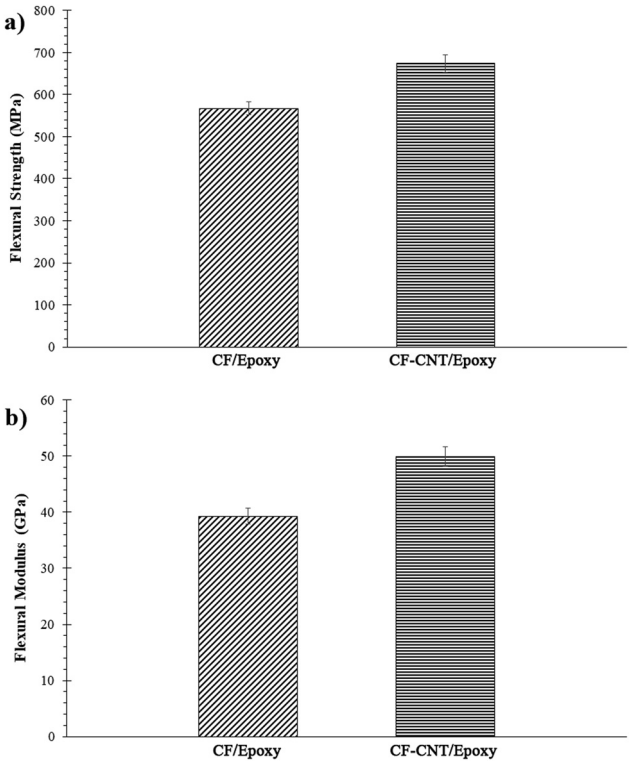

Figure 8: Flexural properties of CF/epoxy and CF–CNT/epoxy in terms of (a) ultimate flexural strength and (b) flexural modulus.

There was also a significant improvement in the flexural modulus of the CF–CNT/epoxy compared to that of the CF/epoxy, as shown in Figure 8b. The overall improvement in the flexural modulus of the CF–CNT/epoxy was 27% (49.9 GPa) above that of the CF/epoxy. Such an improvement could be attributed to the deposition of

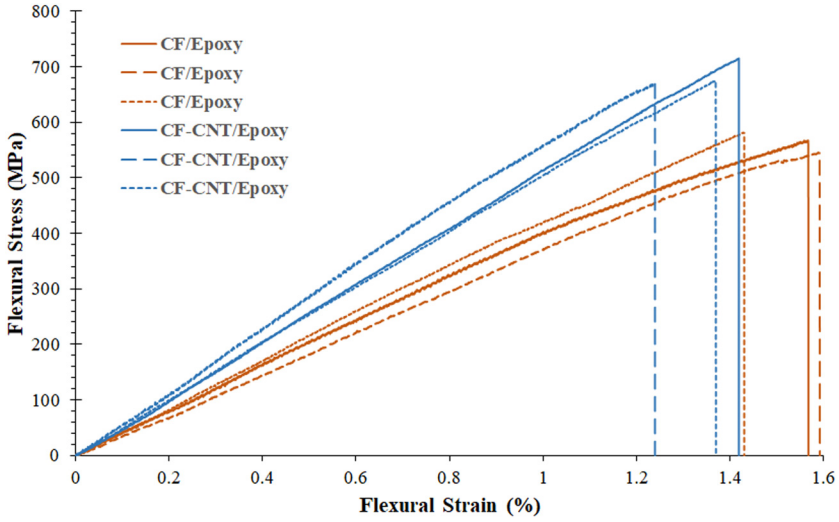

Figure 7: Flexural stress–strain curves of CF/epoxy and CF–CNT/epoxy.

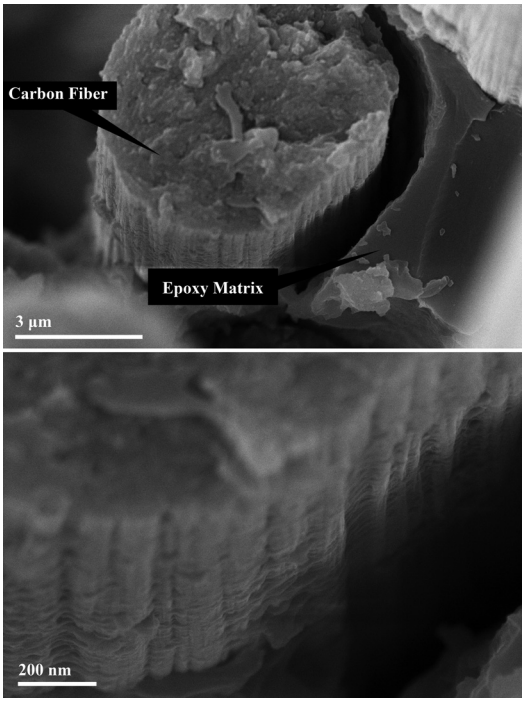

Figure 9: SEM images of the flexural fractured surfaces of CF/epoxy.

CNT, which filled the voids on the woven CF. Generally, there are spaces between the CF tows crossing each other on the woven CF, and these can lead to the trapping of air bubbles during the fabrication of a composite. Thus, the CNT deposition on the woven CF appeared to be accountable for this improvement and also gave rise to interlocking between the CF and the epoxy matrix. The statement was also in agreement with the study by Zhao et al., which reported an increase in flexural modulus of about 27% when using hybrid CF–CNT produced via the EPD method [40]. Based on the literature report, the CNT deposition on the CF surface has a significant impact and is capable of improving the flexural properties of epoxy composite laminates.

The effectiveness of the CF and hybrid CF–CNT as a reinforcement in epoxy composite laminates was determined mainly by their interfacial bonding with the epoxy matrix. For this reason, a morphological characterization was crucial for the evaluation of the interfacial state of the CF and hybrid CF–CNT in the epoxy matrix. Figures 9 and 10 show the morphologies of the flexural fractured surface of the CF/epoxy and CF–CNT/epoxy. As can be seen in Figure 9, the CF had a smooth surface with minimal signs of any interaction between the CF surface and epoxy matrix. In addition, it could be observed that the CF surface was obviously crenulated. In the case of the CF–CNT/epoxy, as shown in Figure 10, it could be seen that there had been some interaction between the hybrid CF–CNT and epoxy matrix. Besides that, the CNT also remained firmly on the CF surface after the fracture. This confirmed that the deposition of CNT on the CF surface helped to create interlocking between the CF and epoxy matrix. Furthermore, the presence of the CNT also increased the interfacial friction and restricted the motion of the epoxy matrix at the interface area. Finally, the CNT played a role in the improvement at the interfacial area by efficiently facilitating the transfer of stress from the matrix to the CF, thereby leading to the enhancement of the flexural properties.

The dielectric constant of CF/epoxy and CF–CNT/epoxy with an increased frequency range from 1 kHz to 1 MHz is shown in Figure 11. As shown in the figure, as the frequency increased, the CF/epoxy and CF–CNT/epoxy show a decrease in the dielectric constant. As is well known, the dielectric constant represents the polarization response to an electrical field and the electric dipoles tend to align with the applied field. The decrease in the dielectric constant with increasing frequency is due to the decrease in total polarization resulting from dipoles. The high rate alteration of electric field at high frequency makes it difficult for dipoles to orient themselves in the direction of the applied field and leads to a low dielectric constant. Meanwhile, at low frequency, the dipoles easily orient themselves in the direction of the applied field at low rate alteration of the electric field and lead to higher dielectric constant.

From the result, CF–CNT/epoxy showed a higher dielectric constant compared to CF/epoxy. The dielectric constant of CF–CNT/epoxy was significantly increased to 364, which corresponded to an increase of 22% compared to CF/epoxy at a frequency of 1 KHz. At a higher frequency of 1 MHz, CF–CNT/epoxy shows the dielectric constant of 355, which corresponded to an increase of 25% compared to CF/epoxy. The high dielectric constant of CF–CNT/epoxy can be attributed mainly to the formation of micro-capacitor network and the effect of interfacial polarization or specifically named Maxwell–Wagner–Sillars (MWS) effect in heterogeneous epoxy composite laminates [43]. Micro-capacitor network formation can be invoked as one of the reasons for such enhancement. The presence of the CNT on the CF surface reduced the isolation distance between each woven CF layer and finally formed more micro-capacitor network. This micro-capacitor network contributes to the abnormally large capacitance, which can then be associated with the significant increase in dielectric constant [44]. The MWS effect can refer to phenomena caused by charge separation at the interface of two mediums with different electrical conductivity and dielectric constant [45]. In the

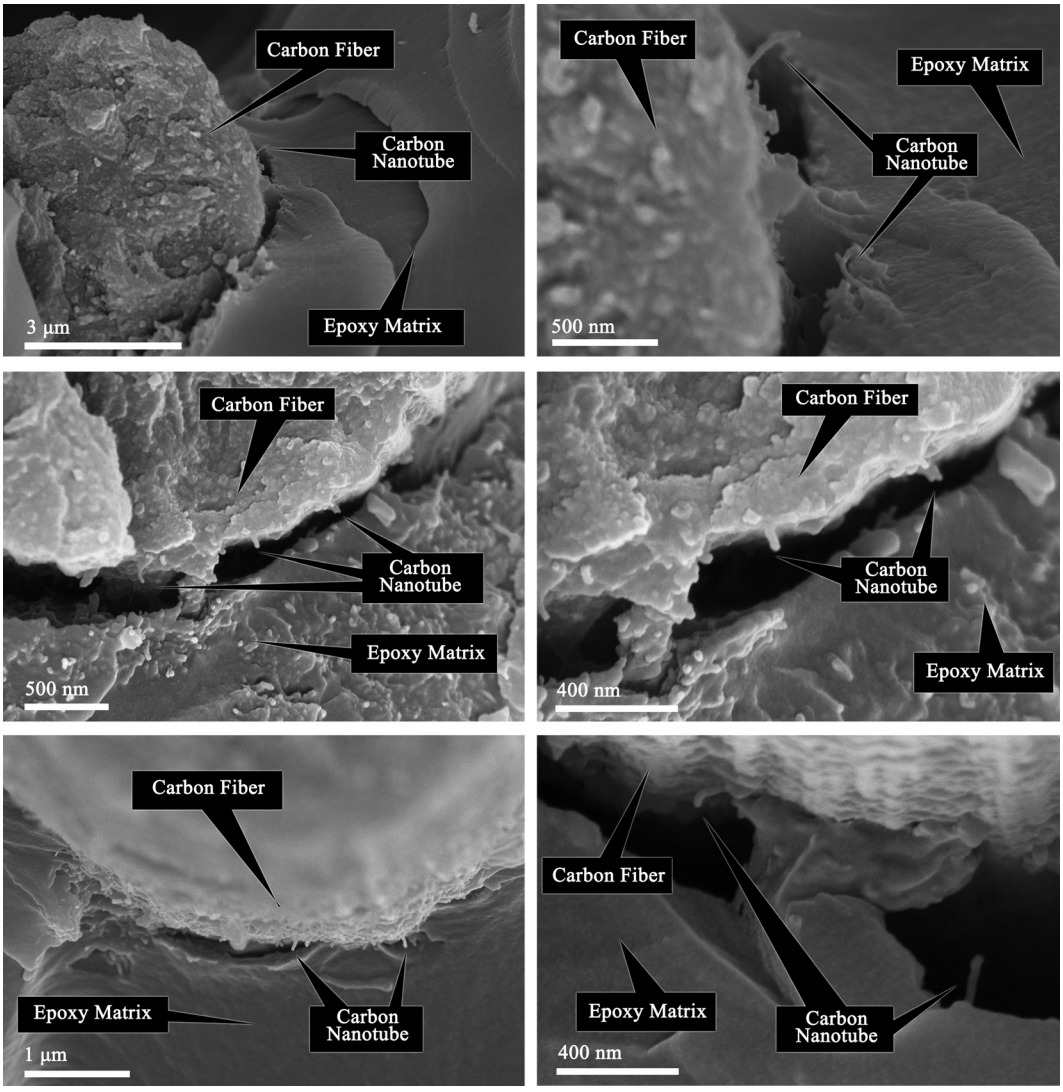

Figure 10: SEM images of the flexural fractured surfaces of CF–CNT/epoxy.

CF–CNT/epoxy system, large specific surface area of CNT deposited on the CF surface has increased the accumulated charge carriers at the interface between the hybrid CF–CNT and the epoxy matrix. This leads to an increase in the polarization of MWS and has resulted in a significant increase in the dielectric constant.

The dielectric loss of CF/epoxy and CF–CNT/epoxy with an increased frequency is shown in Figure 12. From the figure, it can be seen that the CF–CNT/epoxy showed a slightly higher dielectric loss compared to the CF/epoxy. This is due to the presence of highly conductive CNT on the woven CF surface in the epoxy composite laminates. Thus, a leakage current emerged when the epoxy composite laminates became more conductive, converting some of the electrical energy into thermal energy [46].

4 Conclusion

Woven hybrid CF–CNTCF–CNT was prepared by using ESD with an applied voltage of 15 kV and spray duration of 15 min. This method used high-electric field to produce a uniform coating and homogeneous distribution of CNT on the woven CF surface. The woven hybrid CF–CNT epoxy composite laminates were prepared by vacuum-assisted resin transfer moulding with good final samples to ensure the reliability of the test. The flexural strength, flexural modulus and dielectric constant of the woven hybrid CF–CNT epoxy composite laminates were enhanced by about 19, 27 and 25%, respectively compared to the woven CF epoxy composite laminates. Specifically, the improvement in flexural and dielectric properties was also reported to be attributed to the addition of CNT.

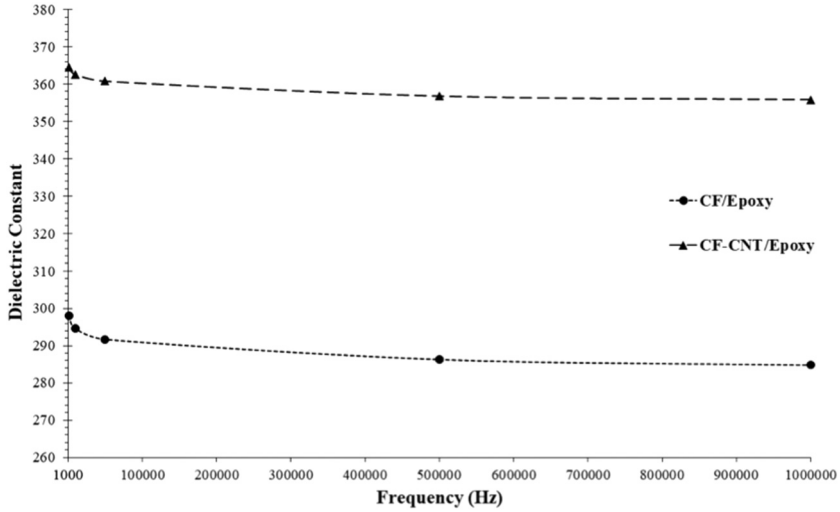

Figure 11: Frequency dependence of the dielectric constants of CF/epoxy and CF–CNT/epoxy.

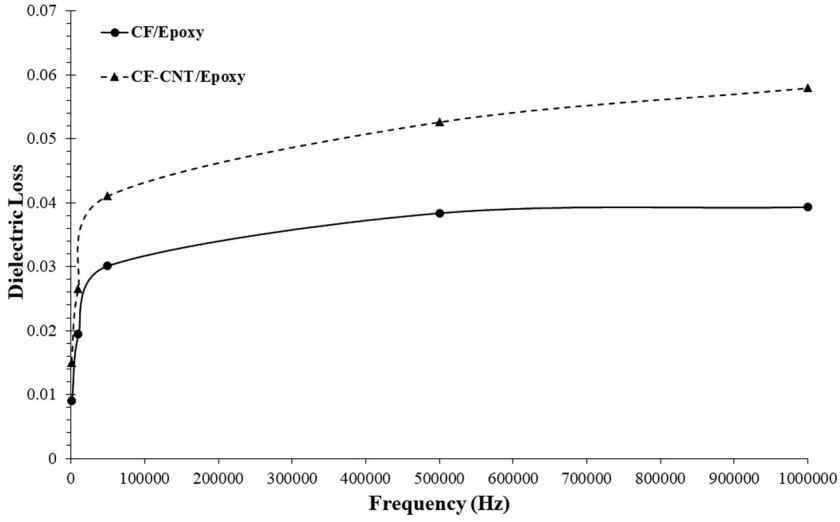

Figure 12: Frequency dependence of the dielectric loss of CF/epoxy and CF–CNT/epoxy.

Based on the morphology observation on the interface, the CNT remained firmly on the CF surface after the fracture, which was the main reason for the improvement of the flexural properties. Meanwhile, the enhancement of dielectric properties is due to the presence of CNT on the woven CF surface, which helps to form more micro-capacitors in epoxy composite laminates. Based on the results, the ESD method provides a new and an effective way to prepare woven hybrid CF–CNT epoxy composite laminates with excellent flexural and dielectric properties. In addition, the ESD method is simple, low cost and suitable for large-scale production compared to chemical vapour deposition and electrophoretic deposition.

Acknowledgments: The authors would like to acknowledge Universiti Sains Malaysia (USM) RUI 1001/PBAHAN/8014047 for sponsoring and providing financial assistance during this research work and Universiti Malaysia Perlis for sponsoring postdoctoral fellowship.

Conflict of interest: The authors declare no conflict of interest regarding the publication of this paper.

References

[1] Islam MS, Deng Y, Tong L, Faisal SN, Roy AK, Minett AI, et al. Grafting carbon nanotubes directly onto carbon fibers for

superior mechanical stability: towards next generation aerospace composites and energy storage applications. Carbon. 2016;96:701–10.
[2] Forintos N, Czigany T. Multifunctional application of carbon fiber reinforced polymer composites: electrical properties of the reinforcing carbon fibers – a short review. Composites Part B. 2019;162:331–43.
[3] Wang C, Li Y, Tong L, Song Q, Li K, Li J, et al. The role of grafting force and surface wettability in interfacial enhancement of carbon nanotube/carbon fiber hierarchical composites. Carbon. 2014;69:239–46.
[4] Yuan X, Zhu B, Cai X, Zhao S, Qiao K, Zhang M. Effects of particle size and distribution of the sizing agent on carbon fiber/epoxy composites interfacial adhesion. Polym Compos. 2018;39(S4):E2036–E45.
[5] Aoife CP, Brian G, Shaneel C, James C. Carbon nanomaterials and their application to electrochemical sensors: a review. Nanotechnol Rev. 2018;7(1):19–41.
[6] Yan M, Liu L, Chen L, Li N, Jiang Y, Xu Z, et al. Radiation resistance of carbon fiber-reinforced epoxy composites optimized synergistically by carbon nanotubes in interface area/matrix. Composites Part B. 2019;172:447–57.
[7] Sang-Youl L, Ji-Gwang H. Finite element nonlinear transient modelling of carbon nanotubes reinforced fiber/polymer composite spherical shells with a cutout. Nanotechnol Rev. 2019;8(1):444–51.
[8] Hanizam H, Mohd Shukor S, Mohd Zaidi O. Homogenous dispersion and interfacial bonding of carbon nanotube reinforced with aluminum matrix composite: a review. Rev Adv Mater Sci. 2019;58(1):295–303.
[9] Lakshman KV, Stephen EC, Apparao MR, Ramakrishna P. Carbon nanotubes coated paper as current collectors for secondary Li-ion batteries. Nanotechnol Rev. 2019;8(1):18–23.
[10] Schilde C, Schlömann M, Overbeck A, Linke S, Kwade A. Thermal, mechanical and electrical properties of highly loaded CNT-epoxy composites – a model for the electric conductivity. Compos Sci Technol. 2015;117:183–90.
[11] Hassanzadeh-Aghdam MK, Mahmoodi MJ, Jamali J, Ansari R. A new micromechanical method for the analysis of thermal conductivities of unidirectional fiber/CNT-reinforced polymer hybrid nanocomposites. Composites Part B. 2019;175:107137.
[12] Chen J, Lekawa-Raus A, Trevarthen J, Gizewski T, Lukawski D, Hazra K, et al. Carbon nanotube films spun from a gas phase reactor for manufacturing carbon nanotube film/carbon fibre epoxy hybrid composites for electrical applications. Carbon. 2020;158:282–90.
[13] Ou Y, González C, Vilatela JJ. Interlaminar toughening in structural carbon fiber/epoxy composites interleaved with carbon nanotube veils. Composites Part A. 2019;124:105477.
[14] Boroujeni AY, Al-Haik M. Carbon nanotube–Carbon fiber reinforced polymer composites with extended fatigue life. Composites Part B. 2019;164:537–45.
[15] Liu Y-T, Yao T-T, Zhang W-S, Wu G-P. Laser welding of carbon nanotube networks on carbon fibers from ultrasonic-directed assembly. Mater Lett. 2019;236:244–7.
[16] Zhang W, Deng X, Sui G, Yang X. Improving interfacial and mechanical properties of carbon nanotube-sized carbon fiber/epoxy composites. Carbon. 2019;145:629–39.
[17] Luo H, Lu H, Qiu J. Carbon fibers surface-grown with helical carbon nanotubes and polyaniline for high-performance electrode materials and flexible supercapacitors. J Electroanal Chem. 2018;828:24–32.
[18] Wang X, Wang C, Wang Z, Wang Y, Lu R, Qin J. Colossal permittivity of carbon nanotubes grafted carbon fiber-reinforced epoxy composites. Mater Lett. 2018;211:273–6.
[19] Zhao M, Meng L, Ma L, Ma L, Yang X, Huang Y, et al. Layer-by-layer grafting CNTs onto carbon fibers surface for enhancing the interfacial properties of epoxy resin composites. Compos Sci Technol. 2018;154:28–36.
[20] Deng Y, Islam MS, Tong L. Effects of grafting strength and density on interfacial shear strength of carbon nanotube grafted carbon fibre reinforced composites. Compos Sci Technol. 2018;168:195–202.
[21] Li Q, Church JS, Naebe M, Fox BL. A systematic investigation into a novel method for preparing carbon fibre–carbon nanotube hybrid structures. Composites Part A. 2016;90:174–85.
[22] Li Q, Church JS, Naebe M, Fox BL. Interfacial characterization and reinforcing mechanism of novel carbon nanotube–carbon fibre hybrid composites. Carbon. 2016;109:74–86.
[23] Su-Xi W, Chin Chong Y, Jiating H, Chao C, Siew Yee W, Xu L. Electrospinning: a facile technique for fabricating functional nanofibers for environmental applications. Nanotechnol Rev. 2016;5(1):51–73.
[24] Sagar R, Roumiana SP, Somenath M. Effect of carbon nanotube (CNT) functionalization in epoxy-CNT composites. Nanotechnol Rev. 2018;7(6):475–85.
[25] Yao Z, Wang C, Qin J, Su S, Wang Y, Wang Q, et al. Interfacial improvement of carbon fiber/epoxy composites using one-step method for grafting carbon nanotubes on the fibers at ultra-low temperatures. Carbon. 2020;164:133–42.
[26] Zheng L, Wang Y, Qin J, Wang X, Lu R, Qu C, et al. Scalable manufacturing of carbon nanotubes on continuous carbon fibers surface from chemical vapor deposition. Vacuum. 2018;152:84–90.
[27] Han L, Li K, Sun J, Song Q, Wang Y. Reinforcing effects of carbon nanotube on carbon/carbon composites before and after heat treatment. Mater Sci Eng A. 2018;735:10–8.
[28] Hur J, Stuart SJ. Raman intensity and vibrational modes of armchair CNTs. Chem Phys Lett. 2017;679:45–51.
[29] Levshov DI, Tran HN, Paillet M, Arenal R, Than XT, Zahab AA, et al. Accurate determination of the chiral indices of individual carbon nanotubes by combining electron diffraction and Resonant Raman spectroscopy. Carbon. 2017;114:141–59.
[30] Chernyak SA, Ivanov AS, Stolbov DN, Egorova TB, Maslakov KI, Shen Z, et al. N-doping and oxidation of carbon nanotubes and jellyfish-like graphene nanoflakes through the prism of Raman spectroscopy. Appl Surf Sci. 2019;488:51–60.
[31] Shi W, Liu H, Dong Z, Mi Z, Shieh SR, Sun X, et al. High pressure study of nitrogen doped carbon nanotubes using Raman spectroscopy and synchrotron X-ray diffraction. Arab J Chem. 2020;13(1):3008–16.
[32] Wang W, Wang C, Yue X, Zhang C, Zhou C, Wu W, et al. Raman spectroscopy and resistance-temperature studies of functionalized multiwalled carbon nanotubes/epoxy resin composite film. Microelectron Eng. 2019;214:50–4.
[33] Bulmer JS, Gspann TS, Barnard JS, Elliott JA. Chirality-independent characteristic crystal length in carbon nanotube

textiles measured by Raman spectroscopy. Carbon. 2017; 115:672–80.
[34] Qiu W, Li Q, Lei Z-K, Qin Q-H, Deng W-L, Kang Y-L. The use of a carbon nanotube sensor for measuring strain by micro-Raman spectroscopy. Carbon. 2013;53:161–8.
[35] Landois P, Pinault M, Huard M, Reita V, Rouzière S, Launois P, et al. Structure in nascent carbon nanotubes revealed by spatially resolved Raman spectroscopy. Thin Solid Films. 2014;568:102–10.
[36] Ţucureanu V, Matei A, Avram AM. FTIR spectroscopy for carbon family study. Crit Rev Anal Chem. 2016;46(6):502–20.
[37] Dang Z-M, Wang L, Zhang L-P. Surface functionalization of multiwalled carbon nanotube with trifluorophenyl. J Nanomater. 2006;2006:5.
[38] Varga M, Izak T, Vretenar V, Kozak H, Holovsky J, Artemenko A, et al. Diamond/carbon nanotube composites: Raman, FTIR and XPS spectroscopic studies. Carbon. 2017;111:54–61.
[39] Yao H, Sui X, Zhao Z, Xu Z, Chen L, Deng H, et al. Optimization of interfacial microstructure and mechanical properties of carbon fiber/epoxy composites via carbon nanotube sizing. Appl Surf Sci. 2015;347:583–90.
[40] Zhao Z, Teng K, Li N, Li X, Xu Z, Chen L, et al. Mechanical, thermal and interfacial performances of carbon fiber reinforced composites flavored by carbon nanotube in matrix/interface. Compos Struct. 2017;159:761–72.
[41] Rahmanian S, Thean KS, Suraya AR, Shazed MA, Salleh MAM, Yusoff HM. Carbon and glass hierarchical fibers: influence of carbon nanotubes on tensile, flexural and impact properties of short fiber reinforced composites. Mater Des. 2013;43:10–6.
[42] Wang C, Li Y, Tong L, Song Q, Li K, Li J, et al. The role of grafting force and surface wettability in interfacial enhancement of carbon nanotube/carbon fiber hierarchical composites. Carbon. 2014;69:239–46.
[43] Chang J, Liang G, Gu A, Cai S, Yuan L. The production of carbon nanotube/epoxy composites with a very high dielectric constant and low dielectric loss by microwave curing. Carbon. 2012;50(2):689–98.
[44] Liu C, Zhang T, Daneshvar F, Feng S, Zhu Z, Kotaki M, et al. High dielectric constant epoxy nanocomposites based on metal organic frameworks decorated multi-walled carbon nanotubes. Polymer. 2020;207:122913.
[45] Xia X, Weng GJ, Hou D, Wen W. Tailoring the frequency-dependent electrical conductivity and dielectric permittivity of CNT-polymer nanocomposites with nanosized particles. Int J Eng Sci. 2019;142:1–19.
[46] Poh CL, Mariatti M, Noor AFM, Sidek O, Chuah TP, Chow SC. Dielectric properties of surface treated multi-walled carbon nanotube/epoxy thin film composites. Compos B Eng. 2016;85:50–8.